Journal of proteome research

pubs.acs.org/jpr

Technical Note

Toward Zero Variance in Proteomics Sample Preparation: Positive-Pressure FASP in 96-Well Format (PF96) Enables Highly Reproducible, Time- and Cost-Efficient Analysis of Sample Cohorts

Stefan Loroch,* Dominik Kopczynski, Adriana C. Schneider, Cornelia Schumbrutzki, Ingo Feldmann, Eleftherios Panagiotidis, Yvonne Reinders, Roman Sakson, Fiorella A. Solari, Alicia Vening, Frauke Swieringa, Johan W. M. Heemskerk, Maria Grandoch, Thomas Dandekar, and Albert Sickmann*

Cite This: *J. Proteome Res.* 2022, 21, 1181−1188

Read Online

ACCESS | Metrics & More | Article Recommendations | Supporting Information

ABSTRACT: As novel liquid chromatography−mass spectrometry (LC-MS) technologies for proteomics offer a substantial increase in LC-MS runs per day, robust and reproducible sample preparation emerges as a new bottleneck for throughput. We introduce a novel strategy for positive-pressure 96-well filter-aided sample preparation (PF96) on a commercial positive-pressure solid-phase extraction device. PF96 allows for a five-fold increase in throughput in conjunction with extraordinary reproducibility with Pearson product-moment correlations on the protein level of r = 0.9993, as demonstrated for mouse heart tissue lysate in 40 technical replicates. The targeted quantification of 16 peptides in the presence of stable-isotope-labeled reference peptides confirms that PF96 variance is barely assessable against technical variation from nanoLC-MS instrumentation. We further demonstrate that protein loads of 36−60 μg result in optimal peptide recovery, but lower amounts ≥3 μg can also be processed reproducibly. In summary, the reproducibility, simplicity, and economy of time provide PF96 a promising future in biomedical and clinical research.

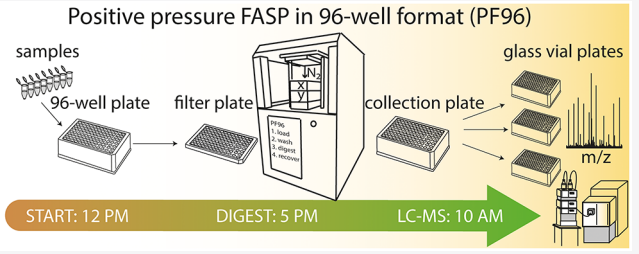

KEYWORDS: *automation, FASP, PF96, proteomics, sample preparation*

INTRODUCTION

With the advent of novel mass spectrometry (MS) acquisition methods for bottom-up proteomics, such as parallel accumulation-serial fragmentation (PASEF),[1] data-independent acquisition (DIA), DIA-PASEF,[2] and BoxCar,[3] the acquisition speed for proteome analyses has substantially increased. In conjunction with improved or novel liquid chromatography (LC) variants, which reduce overhead times to a minimum, a throughput of hundreds of samples per day per LC-MS instrument becomes feasible.[4,5] These novel possibilities for enlarging sample cohort sizes, especially in terms of replicate numbers, can now be exploited to significantly enhance the statistical power in biomedical or clinical research. Consequently, highly robust and time-efficient sample preparation strategies need to be established to prevent sample preparation from becoming a new bottleneck of throughput.

A major challenge in proteomics sample preparation is the removal of the detergent used for cell lysis and protein solubilization. This is usually conducted via precipitation, sodium dodecyl sulphate−polyacrylamide gel electrophoresis (SDS-PAGE), surface immobilization (SP3),[6] or a widely used technique, filter-aided sample preparation (FASP).[7,8] In the latter case, the soluble protein fraction is spun into a molecular weight cutoff (MWCO) filter membrane where proteins are retained, allowing the exchange of the harsh lysis buffer against milder, trypsin-compatible buffers for proteolytic digestion. In particular, when processing larger sample cohorts, manual processing with single FASP spin-tips becomes increasingly time consuming and error prone, as reaction vessels need to be labeled and samples and liquids need to be manually transferred one-by-one. Consequently, sample preparation techniques are increasingly translated to a 96-well format, rendering state-of-the-art liquid-handling platforms increasingly attractive.[9,10]

Because centrifugal force limitations of consumables render a transfer of FASP to 96-well format challenging,[11,12] we introduce a novel positive-pressure-based FASP in 96-well format (PF96), which can be easily conducted using a commercial solid-phase extraction (SPE) unit.[13] In conjunction with liquid-handling support for sample loading, washing, and peptide recovery, it has been embedded into a semiautomated sample preparation pipeline.[14] First, samples are transferred

Received: August 31, 2021
Published: March 22, 2022

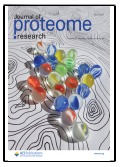

https://doi.org/10.1021/acs.jproteome.1c00706
J. Proteome Res. 2022, 21, 1181−1188

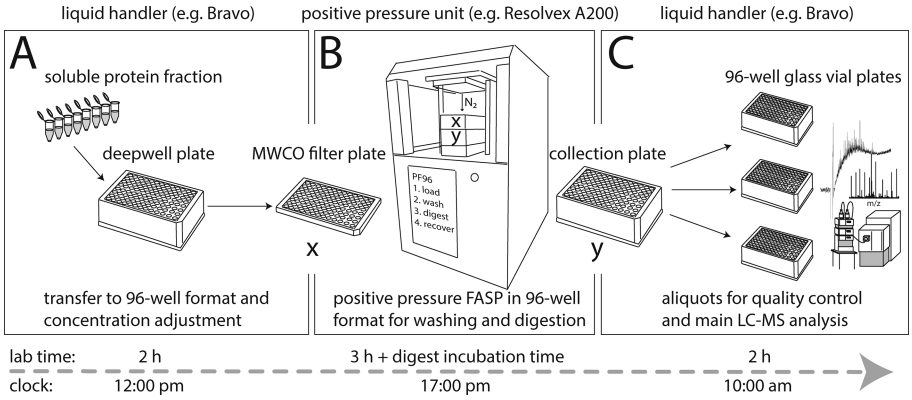

Figure 1. Workflow for semiautomated, positive-pressure filter-aided sample preparation in 96-well format (PF96) using a Resolvex A200 positive-pressure solid-phase extraction unit in conjunction with a Bravo liquid-handling platform. During or after lysis, samples are transferred by a liquid-handling platform (Bravo) to a 96-well format for concentration adjustment, reduction and alkylation followed by transfer to a 96-well MWCO filter plate (A). Proteins are pushed into the filter, washed, and, after digestion, recovered into a 96-well plate by the Resolvex A200's positive-pressure option (B) followed by the transfer of aliquots into 96-well glass vial plates for quality control and LC-MS analysis using a liquid-handling device (C). Notably, because samples keep designated positions during the entire workflow, errors from manual handling are widely omitted.

during or after lysis to a 96-well polypropylene plate, subsequently reduced and alkylated, and loaded onto a 96-well MWCO filter plate (30 kDa) (Figure 1A). Second, liquids during PF96 are forced through the filter by positive pressure, and buffers are added by automatic dispensing followed by enzymatic digestion at 37 °C. Third, peptides are recovered by positive pressure into another 96-well polypropylene plate (Figure 1B), which is also used for sample storage, and aliquots for LC-MS analysis are transferred to 96-well glass vial plates (Figure 1C). Notably, throughout the entire workflow, manual pipetting errors and time-consuming centrifugation steps are widely omitted,[14] and because samples keep their designated 96-well positions, easy tracing of samples, even upon long-term storage, becomes possible.

EXPERIMENTAL PROCEDURES

Preparation of HeLa Cell Lysate

Cells were grown in Dulbecco's modified Eagle's medium (D-MEM, low glucose) supplemented with 10% fetal calf serum (FCS), 4 mM glutamine, 100 U/mL penicillin, and 100 μg/mL streptomycin. Incubation conditions were kept constant at 37 °C and 5% CO_2. Cells were passaged 1:10 or 1:20 every 3 to 4 days at ∼90% confluence, as determined by light microscopy. For harvesting, cells were washed with ice-cold phosphate-buffered saline (PBS) and detached by scraping in the presence of 100 μL of 1% sodium dodecyl sulfate (SDS) per 10^6 cells and transferred to a 15 mL tube followed by homogenization via an ultrasonic probe (10 s cycles, 40 W, three to four repetitions) with incubation on ice in between. After centrifugation for 10 min at 4 °C and 20 000*g*, the clear supernatant was transferred to a new tube, and 10 μL was subjected to concentration determination via amino acid analysis (AAA).[15]

Preparation of Mouse Heart Tissue Lysate

All animals were treated in accordance with federal guidelines according to the Committee on Animal Research of the regional government (Landesamt für Natur, Umwelt and Verbraucherschutz Nordrhein-Westfalen LANUV-NRW Az 81-02.04.2018.A079). Mouse heart tissue samples were prepared from the left ventricular tissue of a PBS/heparin-perfused heart. ∼8 mg of punched tissue was mixed with 300 μL of lysis buffer (50 mM Tris-HCl pH 7.8, 150 mM NaCl, 1% SDS supplemented with cOmplete, mini, EDTA-free protease inhibitor and PhosSTOP (Roche, Penzberg, Germany)). Approximately 20 glass beads were added prior to disruption by sonication for 20 min (30 s on−off cycles) using a Bioruptor Plus sonication device (Diagenode, Liège, Belgium). Ten μL of the homogenate was subjected to AAA.

Amino Acid Analysis

The protein concentration of samples was determined by AAA according to Cohen et al.[15] Proteins were hydrolyzed with 6 M HCl in the gas phase for 2 h at 150 °C, norleucine was added as an internal standard, and 6-aminoquinolyl-*N*-hydrosysuccinimidyl carbamate (AQC, Chemos, Regenstauf, Germany) was used for derivatization to enable fluorescence detection. Quantification was conducted against an eight-point calibration curve of AQC-derivatized amino acids in the range from 1 to 50 pmol/μL using a Vanquish Horizon ultra-high-performance liquid chromatography (UHPLC) apparatus (Thermo Fisher, Bremen, Germany) for separation.

PF96

Cysteines were reduced using 10 mM dithiothreitol at 56 °C for 30 min and alkylated in the presence of 20 mM iodoacetamide for 30 min at room temperature (RT) in the dark. Samples were diluted at least 1:4 in 8 M urea dissolved in 150 mM Tris-HCl, pH 8.5 and transferred to a 30 kDa AcroPrep Omega filter membrane plate (Pall, Port Washington, New York; purchased via VWR, Hannover, Germany, REF 8035/518-0028). The filter plate was placed on top of a 2.2 mL MegaBlock collection plate (Sarstedt, Nümbrecht, Germany), and the liquid of the protein solution was forced through the filter using a Resolvex A200 apparatus (Tecan, Männedorf, Switzerland) connected to nitrogen gas (N_2, 5.5 bar, purity 4.8 or higher; Linde, Düsseldorf, Germany) using a relative pressure of 20% of the low-profile setting. Subsequently, the dispensing function of the A200 was used to wash the filter twice with 200 μL of 8 M urea buffer in 150 mM Tris-HCl pH 8.5 and twice with 200 μL of 50 mM ammonium bicarbonate (ABC). After each washing step, the liquid was forced through the filter using the same pressure profile as for loading. In most cases, 30 min of pressure were sufficient; however, in the case of residual liquid, positive pressure was applied for an additional 15 min. Afterward, the plate was centrifuged for 2 min at 2000*g* to remove residual

https://doi.org/10.1021/acs.jproteome.1c00706
J. Proteome Res. 2022, 21, 1181−1188

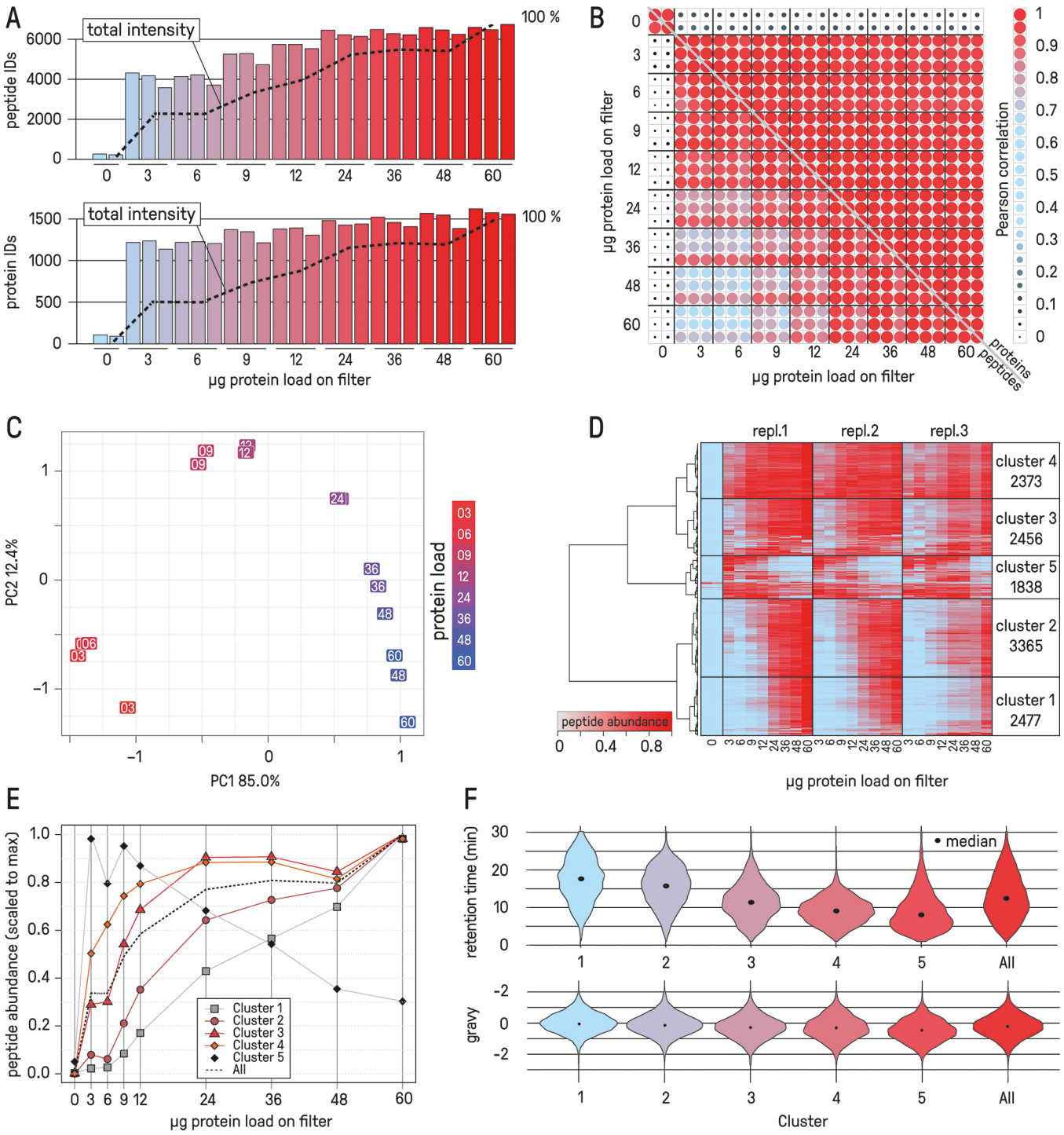

Figure 2. PF96 with varying protein loads (triplicates) to mimic experiments with limited sample amounts or low-concentration samples followed by LC-MS using 100 ng (theoretical peptide concentration). The processing of lower protein loads (3−6 μg) results in a quantitative loss of ∼60%, whereas sample amounts of 36−60 μg allow for maximal recovery with respect to the total signal intensity (dashed line), a trend that is somewhat less pronounced on the peptide and protein ID level level (A). The Pearson correlation matrix displays an excellent correlation for equal sample amounts but poor correlation for varying loads (B), emphasizing that peptide stoichiometry is altered. Accordingly, principal component analysis displays a clear separation of low and high protein loads within the first two components, explaining 97% of the variance (C). Hierarchical clustering analysis unveiled two peptide clusters (comprising 47% of all peptides) with clearly diminished intensities for lower protein loads (D,E). Those clusters predominantly comprise peptides of higher retention in ion-pairing reversed-phase nanoLC but no appreciable difference in the GRAVY index according to Kyte and Doolitle (F).[21]

drops, which sometimes remain under the membrane. For digestion, 100 μL of digestion buffer was added comprising 100 mM urea, 50 mM ABC, and 1 mM $CaCl_2$ including sequencing-grade trypsin (Promega, sequencing-grade-modified trypsin, Madison, Wisconsin) in a concentration to meet a 1:33 enzyme-to-sample ratio. After incubation for 15 h at 37 °C, the digested protein fraction was forced through the filter and collected in a 500 μL LoBind plate (Eppendorf, Hamburg, Germany). 20−50

https://doi.org/10.1021/acs.jproteome.1c00706
J. Proteome Res. 2022, 21, 1181−1188

μL aliquots were transferred to 700 μL glass-vial plates (Waters, Eschborn, Germany) using a Bravo liquid-handling system (Agilent, Waldbronn, Germany) for injection in a monolithic column-HPLC (quality control)[16] and nanoLC-MS/MS.

LC-MS in Data-Dependent Acquisition Mode

LC-MS was conducted using a U3000 RSLCnano ProFlow system online-coupled to a Q Exactive HF mass spectrometer (both Thermo Scientific, Dreieich, Germany, including HPLC columns). Employed solvents were LC-MS grade or higher (Biosolve, Valkenswaard, Netherlands). Samples were loaded in 0.1% trifluoroacetic acid (TFA) at a flow rate of 30 μL/min onto a trap column (Acclaim PepMap C18, 0.1 × 20 mm, 5 μm, 100 Å) for online SPE to remove remaining salts from the digestion. After 5 min, the trap column was switched in line with the main column (Acclaim PepMap C18, 0.075 × 500 mm, 2 μm, 100 Å), and peptides were separated using a binary acetonitrile (ACN) gradient in the presence of 0.1% formic acid at 60 °C and a flow rate of 250 nL/min. In the case of HeLa protein load ladders, a 35 min binary gradient ranging from 4 to 34% (ACN) was used and, in the case of heart tissue experiments, a 65 min binary gradient from 6 to 32% ACN. The MS was operated in data-dependent acquisition (DDA) mode with survey scans acquired at a resolution of 60 000 followed by 15 MS/MS scans at a resolution of 15 000 (top15). Precursor ions were selected for MS/MS by intensity, isolated in a 1.6 m/z window, and subjected to fragmentation by higher energy-collision-induced dissociation using a normalized collision energy (NCE) of 27. Automatic gain control (AGC) target values were set to 10^6 and 5×10^4, and the maximum ion injection was set to 120 and 50 ms for MS and MS/MS, respectively. Precursor masses were excluded from refragmentation for 20 s (dynamic exclusion), and the polysiloxane at m/z 371.1012 was used as an internal calibrant.[17]

Short-Gradient-Targeted LC-MS in Parallel Reaction Monitoring Mode

For targeted LC-MS, 2.5 μL of mouse heart digest with an estimated concentration of 75 ng/μL was injected including 22 stable-isotope-labeled (SIL) peptides ranging from 0.5 to 50 fmol/μL. Samples were loaded in 0.1% TFA at flow rate of 100 μL/min, and the precolumn (Acclaim PepMAP C18, 0.3 × 5 mm, 5 μm, 100 Å) was switched in-line after 30 s. Peptides were separated at a flow rate of 500 nL/min (Acclaim PepMAP C18, 0.075 × 150 mm, 2 μm, 100 Å) using a 12 min linear ACN gradient from 4 to 25% ACN in the presence of 0.1% FA. The Q Exactive HF apparatus was operated in parallel reaction monitoring (PRM) mode using a resolution of 60 000 (at 200 m/z) and a maximum ion injection time of 120 ms to reach the AGC target value of 10^6. Corresponding heavy and light precursor ions were isolated using a 0.4 m/z window and fragmented using an NCE of 27. Peptides were triggered in a 1.5 min window at their expected retention time (scheduled mode), resulting in 10 parallel precursors maximum.

Data Analysis for DDA

DDA files were processed with Proteome Discoverer 2.3 (Thermo Scientific, Bremen, Germany) using Mascot 2.6 (Matrix Science, London, U.K.) as the database search algorithm and Percolator[18] in conjunction with Peptide validator to adjust the false discovery rate to 1% on the peptide-spectrum match (PSM) and peptide level. Quantification was exclusively performed with unique peptides using the Minora feature detector in conjunction with the feature mapper node with disabled scaling and normalization. A database search was conducted against UniProt mouse (Sept 2019, 17 027 target sequences) or human (July 2018, 20 385 target sequences) with error tolerances of 10 ppm and 0.02 Da for precursor and fragment ions and the following settings: trypsin as the enzyme, oxidation of Met as the variable modification (+15.9949 Da), and carbamidomethylation of Cys (+57.0214 Da) as the fixed modification. Peptide result tables were exported and further processed in Microsoft Excel 2016 and R v3.6.3. Pearson product-moment correlation matrices were generated using the corrplot function of the corrplot package v0.84 and were further used as a distance matrix for principal component analyses (PCAs). Hierarchical clustering was performed using the hclust basic function with Manhattan distance and ward.D clustering of the heatmap.2 function of the gplots package v3.0.4. Violin plots were generated using the ggplot2 package v3.3.2, whereas all other plots were generated using basic R functions. Base peak intensities were plotted with the package rawDiag v0.0.34,[19] KEGG Mapper (www.genome.jp/kegg/tool/conv_id.html) was used for identifier conversion, and the pathview package v1.26.0 was used for generating pathway maps.[20]

Data Analysis for PRM

Raw files were imported into Skyline v19.1 and three to five of the best transitions were selected for quantification, except for the endogenous peptide DVKPSNILVNSR, which could only be detected with two transitions. The "peptide ratio result" export function was used to export ratios to SIL and endogenous peptide areas. Further processing was done in R v3.6.3 using the ggplot2 package v3.3.2 to generate violin plots and basic R-functions for bar and scatter plots. The 2D contour plots were rendered using the matplotlib module in Python 3.8. Additionally, we used kernel density estimation (KDE, which is a nonparametric function) provided within the pandas module in Python. For each dimension (ratios or peak areas of liquid chromatography−mass spectrometry (LCMS) replicates vs PF96 replicates), we generated the corresponding 1D KDE points. The final plots were generated by connecting each 1D plot pair using a Cartesian product.

RESULTS

For our first test, we loaded varying amounts of HeLa and mouse heart tissue lysate onto the filter. PF96 demonstrates excellent reproducibility for similar protein loads over the entire range of 3−60 μg (Figure 2A,B). Importantly, peptide recovery estimations via MS intensities reveal high protein loads (36−60 μg) to yield more peptide IDs (+50%) and higher overall signal intensities (+150%) when a constant amount of 100 ng is injected (calculated concentration according to protein load). Peptide recovery rates over protein loads follow a sigmoid curve, rendering protein loads of ≥36 μg as favorable (Figure 2A). The correlation analysis of samples displays diminished correlation coefficients with increasing differences in protein loads, down to $r = 0.5$ for 3 versus 60 μg (Figure 2B), indicating a substantial alteration of peptide stoichiometry. Accordingly, PCA clearly separates low and high protein loads within the first two principal components (explaining 97% of variance), underscoring the bias in peptide recovery (Figure 2C). In contrast, similar protein loads, which exhibit higher correlation coefficients, cluster together in PCA (Figure 2B,C). Hierarchical clustering of peptides according to intensities revealed five clusters of different responses to protein load variations (Figure 2D,E). Peptides of clusters 1 and 2, which display poor signal

https://doi.org/10.1021/acs.jproteome.1c00706
J. Proteome Res. 2022, 21, 1181−1188

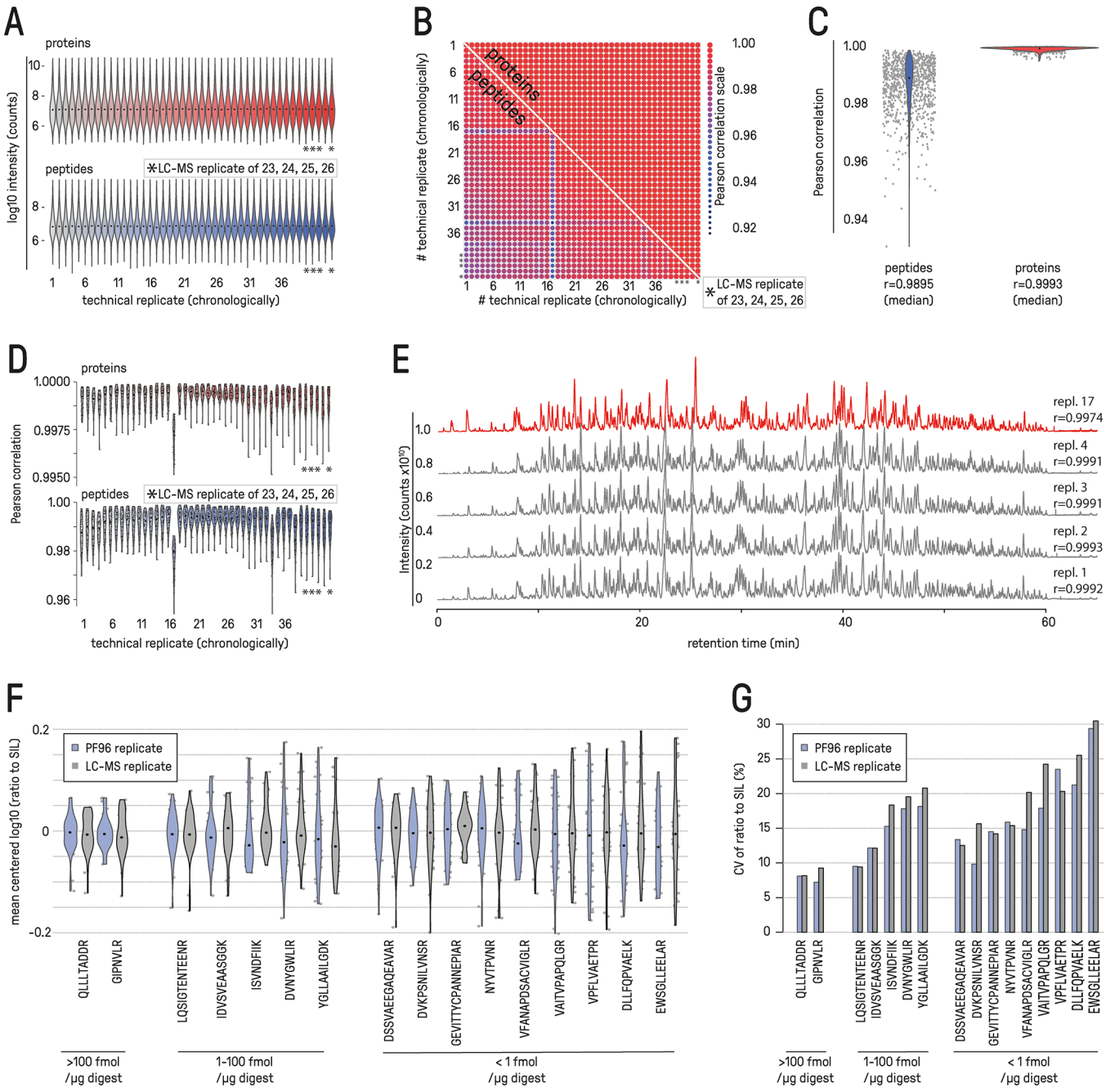

Figure 3. (A–E) PF96 evaluated by shotgun proteomics of mouse heart tissue in 40 technical replicates including four replicate injections to assess variance originating from LC-MS (asterisks indicate reinjections of the PF96 replicates 23–26). Violin plots of protein and peptide intensities display equal peptide recovery rates across all samples (A) with median Pearson product-moment correlation coefficients of $r = 0.9993$ on the protein level and $r = 0.9895$ on the peptide level (B,C). The plot of sample-specific correlation coefficients reveals PF96 variance to be in the range of LC-MS variance for reinjections (D). Visualization of the base peak intensities of replicates 1–4 and 17 (lowest correlation of all, red trace) displays high reproducibility over all samples (E). (F,G) Targeted analysis of 40 PF96 replicates against 40 aliquots of a sample pool shows that the sample preparation variance is not assessable against the LC-MS variance when analyzing log10 ratios to SIL peptides (F) or coefficients of variation (CVs) (G). The 16 target peptides selected span more than four orders of magnitude in abundance. For plotting, peptides were grouped according to abundance and sorted by CV.

intensity with low protein loads, are well-retained by reversed-phase LC and comprise higher shares of the hydrophobic amino acids F, L, M, and W (Figures S1 and S2) but do not display higher GRAVY (grand average of hydropathicity) values (Figure 2 F, Figure S3).[21] With respect to application, the loss of these peptide subsets especially affects the detection of endomembrane-system-related proteins, as visualized by mapping log2 ratios of 3 versus 60 μg[20] to the KEGG pathway "protein processing in endoplasmic reticulum" (www.kegg.jp, mmu04141, Figure S4). In contrast, proteins related to the "MAPK Signalling Pathway" appeared to be less affected by variations in the protein load (www.kegg.jp, mmu04010, Figure S5).

In the next experiment, we wanted to address variance of sample preparation. Hence 48 μg of mouse heart tissue lysate was processed in 40 technical replicates and evaluated by the

https://doi.org/10.1021/acs.jproteome.1c00706
J. Proteome Res. 2022, 21, 1181−1188

following criteria: (1) Pearson correlation in DDA, (2) quantification of 16 endogenous peptides (spanning four orders of magnitude in abundance) by targeted LC-MS, and (3) quantification of the same 16 endogenous peptides against stable-isotope-labeled reference peptides by targeted LC-MS. Upon DDA analysis, 1552 ± 25 proteins (1352 ± 17 with ≥2 unique peptides) and 8952 ± 173 peptides were identified in each replicate, enabling the quantification of 11 094 peptide features (of 16 281 features) with constant signal intensities over all LC-MS runs (Figure 3A). Most notably, the median correlation coefficients were r = 0.9993 and 0.9895 on the protein and peptide level, respectively—extremely close to the median correlation coefficients for replicate injections of single samples (N = 4), which were determined to be r = 0.9994 and 0.9898, respectively (Figure 3B−D). Notably, 1 out of 40 samples exhibited a slightly lower correlation of r = 0.9974 on the protein level (sample 17), but a visual inspection of the base peak chromatogram unveiled only minor differences from other runs (Figure 3B,D,E, Figure S6).[19]

To further address the contribution of PF96 to the overall variance of proteome analyses, we set up a 21 min targeted assay (12 min MS acquisition time) for all 40 mouse heart replicates, which were measured in direct comparison to 40 aliquots of a mouse heart digest pool. Quantification was conducted in the presence of a SIL peptide mixture, and heavy/light pairs of 16 peptides were targeted by PRM in scheduled mode (1.5 min windows, Q Exactive HF, Figure S7). Analysis of the endogenous peptide area irrespective of SIL peptides revealed coefficients of variation (CVs) of 14.8% for the sample pool and 19.2% for PF96 replicates, indicating that a share of 23% of variance originates from PF96 (Figures S8 and S9). In comparison, analysis of endogenous-to-SIL peptide ratios resulted in CVs of 17.3% for sample pool aliquots and 15.6% for PF96 replicates, indicating a sample preparation variance that is indistinguishable from LC-MS variance (Figure 3F,G and Figures S8 and S10). Taken together, DDA and targeted experiments of 40 sample preparation replicates highlight that PF96 gives only a minor and barely assessable contribution to the overall variance of proteomics analyses.

DISCUSSION

PF96 as a combination of FASP with positive-pressure SPE displays excellent robustness and highest reproducibility. The chance of membrane rupture is substantially reduced in comparison with spin filters in conjunction with fixed-angle rotor centrifuges, which apply lateral force, resulting in considerable shear stress. The gain in reproducibility using positive pressure is most likely attributed to the homogeneous force applied to the entire membrane, whereas fixed-angle rotor centrifuges apply pressure to a distinct membrane spot opposite of the rotor axis (visualized with trypan blue solution, Figure S11). In consequence, positive pressure enables more thorough washing of the protein because it is distributed among the entire membrane. Interestingly, positive pressure also does not lead to a loss of additional proteins or larger proteins during loading and washing, which might be a consequence of the pore size or shape changes. We even detected slightly fewer proteins of >30 kDa in the flow through (loading 50 μg of purified platelet protein) in comparison with spin filters with a fixed-angle rotor centrifuge (Figure S12). In comparison with the flow-through when using a swing bucket rotor centrifuge, we detected a very similar protein fraction as in PF96 (Figure S12). Hence, as already described in previous studies, swing bucket rotors offer a valuable alternative to positive pressure but suffer from the force limitations of the consumables, which is usually 2000−6000g (depending on the vendor and the quality of the consumables). Hence, extended centrifugation times or buffer substitutions are mandatory when aiming at the time-economic processing of protein amounts in the middle microgram range.[11,12]

Another advantage represents the SPE unit's automated dispensing function, allowing for the significant reduction of lab time and pipetting errors. This renders costly liquid-handling devices unnecessary. Nevertheless, combinations with liquid-handling devices are beneficial toward the automation of the entire sample preparation pipeline, including the initial sample transfer, concentration adjustment, derivatization steps, and generation of aliquots for analysis. When employing trap-column-based LC systems, allowing for the removal of digestion buffer salts (as in this study), an additional offline SPE step is not mandatory, which reduces lab time and perhaps technical variance even further. An additional gain in time efficiency might be realized in the future via combinations with ultrasonic enhanced digestion.[22] In addition, combinations with emerging 96-well posttranslational modification (PTM) enrichment procedures[23,24] are of particular interest because such workflows rely on highly robust sample preparation.[25]

PF96 demonstrated optimal peptide recovery with protein loads of 36−60 μg. Nevertheless, processing of lower amounts can be performed with high reproducibility at the expense of diminished peptide recovery. The most prominent sources of peptide loss are the surfaces of pipet tips, polypropylene plate walls, and MWCO filter membranes. In addition, because the processing of minute amounts results in low concentrated peptide fractions, the higher required LC injection volumes also contribute to this phenomenon. We demonstrate this by injecting equal amounts of HeLa digest in different concentrations into nanoLC-MS, which displays a similar loss of well-retained peptides, just far less pronounced than that observed for PF96 with low protein loads (Figure S13). Such immobilization processes might be further omitted by the addition of polyvinylpyrrolidone[26] or TWEEN-20[27] to the buffers and by the introduction of more sensitive LC column architectures.[28] However, because surface immobilization processes are not fully understood and are challenging to control, there is a critical need to find adequate materials or surface modifications to reduce losses upon the handling of minute sample amounts. This is especially interesting in light of the emerging attempts to analyze single-cell proteomes.[29]

CONCLUSIONS

PF96 offers low-variance sample preparation and increased throughput with the potential to processes several hundreds of samples per week. The time economy renders it a perfect combination with novel short gradient LC-MS to enhance the throughput capabilities of laboratories. The low variance improves the statistical significance and the reliability of results, rendering PF96 interesting not only for biomarker research and systems biology but also especially for future clinical proteomics applications (e.g., analyses of biopsy samples).

ASSOCIATED CONTENT

Supporting Information

The Supporting Information is available free of charge at https://pubs.acs.org/doi/10.1021/acs.jproteome.1c00706.

https://doi.org/10.1021/acs.jproteome.1c00706
J. Proteome Res. 2022, 21, 1181−1188

Supplemental File 1. Thirteen additional figures supporting the described experiments (PDF)

Supplemental File 2. R and Python scripts including data import tables (ZIP)

Supplemental Table 1. Protein and peptide tables for HeLa ladder experiment 3−60 μg (displayed in Figure 2) (XLSX)

Supplemental Table 2. Protein and peptide tables for 40 replicates (displayed in Figure 3) (XLSX)

AUTHOR INFORMATION

Corresponding Authors

Stefan Loroch − *Leibniz-Institut für Analytische Wissenschaften - ISAS - e.V., 44139 Dortmund, Germany;* orcid.org/0000-0002-7758-0301; Email: Stefan.Loroch@isas.de

Albert Sickmann − *Leibniz-Institut für Analytische Wissenschaften - ISAS - e.V., 44139 Dortmund, Germany; Medizinisches Proteom-Center, Ruhr-Universität Bochum, 44801 Bochum, Germany; Department of Chemistry, College of Physical Sciences, University of Aberdeen, AB24 3FX Aberdeen, United Kingdom;* orcid.org/0000-0002-2388-5265; Email: sickmann@isas.de

Authors

Dominik Kopczynski − *Leibniz-Institut für Analytische Wissenschaften - ISAS - e.V., 44139 Dortmund, Germany*

Adriana C. Schneider − *Leibniz-Institut für Analytische Wissenschaften - ISAS - e.V., 44139 Dortmund, Germany; Faculty of Biochemical and Chemical Engineering, Technical University of Dortmund, 44227 Dortmund, Germany*

Cornelia Schumbrutzki − *Leibniz-Institut für Analytische Wissenschaften - ISAS - e.V., 44139 Dortmund, Germany*

Ingo Feldmann − *Leibniz-Institut für Analytische Wissenschaften - ISAS - e.V., 44139 Dortmund, Germany*

Eleftherios Panagiotidis − *Leibniz-Institut für Analytische Wissenschaften - ISAS - e.V., 44139 Dortmund, Germany*

Yvonne Reinders − *Leibniz-Institut für Analytische Wissenschaften - ISAS - e.V., 44139 Dortmund, Germany*

Roman Sakson − *Leibniz-Institut für Analytische Wissenschaften - ISAS - e.V., 44139 Dortmund, Germany;* orcid.org/0000-0002-9698-0773

Fiorella A. Solari − *Leibniz-Institut für Analytische Wissenschaften - ISAS - e.V., 44139 Dortmund, Germany*

Alicia Vening − *Department of Biochemistry, Cardiovascular Research Institute Maastricht (CARIM), Maastricht University, 6200 MD Maastricht, The Netherlands*

Frauke Swieringa − *Department of Biochemistry, Cardiovascular Research Institute Maastricht (CARIM), Maastricht University, 6200 MD Maastricht, The Netherlands*

Johan W. M. Heemskerk − *Department of Biochemistry, Cardiovascular Research Institute Maastricht (CARIM), Maastricht University, 6200 MD Maastricht, The Netherlands*

Maria Grandoch − *Institut für Pharmakologie und Klinische Pharmakologie, Universitätsklinikum der Heinrich-Heine-Universität Düsseldorf, 40225 Düsseldorf, Germany*

Thomas Dandekar − *Department of Bioinformatics, Biocenter, University of Würzburg, 97074 Würzburg, Germany;* orcid.org/0000-0003-1886-7625

Complete contact information is available at: https://pubs.acs.org/10.1021/acs.jproteome.1c00706

Author Contributions

S.L. contributed to conceptualization, performed experiments, manuscript writing, data analysis and manuscript revision. D.K. and T.D. performed data analysis including statistics, revised the manuscript, and performed experiments and data analysis for revision. A.C.S., C.S., I.F., E.P., F.A.S., and R.S. contributed by conceptualization and performed experiments. A.V., F.S., J.W.M.H., and M.G. contributed by conceptualization, provided biological samples, and revised the manuscript. Y.R. performed experiments and data analysis for revision. A.S. contributed by conceptualization, manuscript writing, and manuscript revision.

Notes

The authors declare no competing financial interest.

All data can be accessed via PRIDE[30] (identifier: PXD024236) and PanoramaWeb[31] (https://panoramaweb.org/LorochPF96.url).

ACKNOWLEDGMENTS

This project was funded by the TRR240 (project Z02) and the SFB1116 (project B10 and S01) of the Deutsche Forschungsgemeinschaft (DFG). Further funding was provided by the Bundesministerium für Bildung und Forschung (BMBF) and by the Ministerium für Kultur und Wissenschaft des Landes Nordrhein-Westfalen (MKW) as well as the Regierender Bürgermeister von Berlin. We further thank Konstantin Shuvaev, Susanne Krois, and Dr. Daniel Krahn from ISAS for the support with peptide synthesis, amino acid analysis, and valuable discussion.

REFERENCES

(1) Meier, F.; Beck, S.; Grassl, N.; Lubeck, M.; Park, M. A.; Raether, O.; Mann, M. Parallel Accumulation-Serial Fragmentation (PASEF): Multiplying Sequencing Speed and Sensitivity by Synchronized Scans in a Trapped Ion Mobility Device. *J. Proteome Res.* **2015**, *14* (12), 5378−87.

(2) Meier, F.; Brunner, A. D.; Frank, M.; Ha, A.; Bludau, I.; Voytik, E.; Kaspar-Schoenefeld, S.; Lubeck, M.; Raether, O.; Bache, N.; Aebersold, R.; Collins, B. C.; Röst, H. L.; Mann, M. diaPASEF: parallel accumulation-serial fragmentation combined with data-independent acquisition. *Nat. Methods* **2020**, *17* (12), 1229−1236.

(3) Meier, F.; Geyer, P. E.; Virreira Winter, S.; Cox, J.; Mann, M. BoxCar acquisition method enables single-shot proteomics at a depth of 10,000 proteins in 100 minutes. *Nat. Methods* **2018**, *15* (6), 440−448.

(4) Bekker-Jensen, D. B.; Martínez-Val, A.; Steigerwald, S.; Rüther, P.; Fort, K. L.; Arrey, T. N.; Harder, A.; Makarov, A.; Olsen, J. V. A Compact Quadrupole-Orbitrap Mass Spectrometer with FAIMS Interface Improves Proteome Coverage in Short LC Gradients. *Molecular & cellular proteomics: MCP* **2020**, *19* (4), 716−729.

(5) Bache, N.; Geyer, P. E.; Bekker-Jensen, D. B.; Hoerning, O.; Falkenby, L.; Treit, P. V.; Doll, S.; Paron, I.; Müller, J. B.; Meier, F.; Olsen, J. V.; Vorm, O.; Mann, M. A Novel LC System Embeds Analytes in Pre-formed Gradients for Rapid, Ultra-robust Proteomics. *Molecular & cellular proteomics: MCP* **2018**, *17* (11), 2284−2296.

(6) Hughes, C. S.; Foehr, S.; Garfield, D. A.; Furlong, E. E.; Steinmetz, L. M.; Krijgsveld, J. Ultrasensitive proteome analysis using paramagnetic bead technology. *Molecular systems biology* **2014**, *10* (10), 757.

(7) Manza, L. L.; Stamer, S. L.; Ham, A. J.; Codreanu, S. G.; Liebler, D. C. Sample preparation and digestion for proteomic analyses using spin filters. *Proteomics* **2005**, *5* (7), 1742−5.

(8) Wisniewski, J. R.; Zougman, A.; Nagaraj, N.; Mann, M. Universal sample preparation method for proteome analysis. *Nat. Meth* **2009**, *6* (5), 359−362.

(9) Hughes, C. S.; Moggridge, S.; Müller, T.; Sorensen, P. H.; Morin, G. B.; Krijgsveld, J. Single-pot, solid-phase-enhanced sample preparation for proteomics experiments. *Nature protocols* **2019**, *14* (1), 68−85.
(10) Chen, Y.; Guenther, J. M.; Gin, J. W.; Chan, L. J. G.; Costello, Z.; Ogorzalek, T. L.; Tran, H. M.; Blake-Hedges, J. M.; Keasling, J. D.; Adams, P. D.; García Martín, H.; Hillson, N. J.; Petzold, C. J. Automated ″Cells-To-Peptides″ Sample Preparation Workflow for High-Throughput, Quantitative Proteomic Assays of Microbes. *J. Proteome Res.* **2019**, *18* (10), 3752−3761.
(11) Yu, Y.; Bekele, S.; Pieper, R. Quick 96FASP for high throughput quantitative proteome analysis. *Journal of proteomics* **2017**, *166*, 1−7.
(12) Potriquet, J.; Laohaviroj, M.; Bethony, J. M.; Mulvenna, J. A modified FASP protocol for high-throughput preparation of protein samples for mass spectrometry. *PloS one* **2017**, *12* (7), e0175967.
(13) Schelletter, L.; Hertel, O.; Antar, S. J.; Scherling, C.; Lättig, J.; Noll, T.; Hoffrogge, R. A positive pressure workstation for semi-automated peptide purification of complex proteomic samples. *Rapid communications in mass spectrometry: RCM* **2021**, *35* (2), e8873.
(14) Kong, F.; Yuan, L.; Zheng, Y. F.; Chen, W. Automatic liquid handling for life science: a critical review of the current state of the art. *Journal of laboratory automation* **2012**, *17* (3), 169−85.
(15) Cohen, S. A.; Michaud, D. P. Synthesis of a fluorescent derivatizing reagent, 6-aminoquinolyl-N-hydroxysuccinimidyl carbamate, and its application for the analysis of hydrolysate amino acids via high-performance liquid chromatography. *Anal. Biochem.* **1993**, *211* (2), 279−87.
(16) Burkhart, J. M.; Schumbrutzki, C.; Wortelkamp, S.; Sickmann, A.; Zahedi, R. P. Systematic and quantitative comparison of digest efficiency and specificity reveals the impact of trypsin quality on MS-based proteomics. *Journal of proteomics* **2012**, *75* (4), 1454−62.
(17) Olsen, J. V.; de Godoy, L. M.; Li, G.; Macek, B.; Mortensen, P.; Pesch, R.; Makarov, A.; Lange, O.; Horning, S.; Mann, M. Parts per million mass accuracy on an Orbitrap mass spectrometer via lock mass injection into a C-trap. *Molecular & cellular proteomics: MCP* **2005**, *4* (12), 2010−21.
(18) Kall, L.; Canterbury, J. D.; Weston, J.; Noble, W. S.; MacCoss, M. J. Semi-supervised learning for peptide identification from shotgun proteomics datasets. *Nat. Methods* **2007**, *4* (11), 923−5.
(19) Trachsel, C.; Panse, C.; Kockmann, T.; Wolski, W. E.; Grossmann, J.; Schlapbach, R. rawDiag: An R Package Supporting Rational LC-MS Method Optimization for Bottom-up Proteomics. *J. Proteome Res.* **2018**, *17* (8), 2908−2914.
(20) Luo, W.; Brouwer, C. Pathview: an R/Bioconductor package for pathway-based data integration and visualization. *Bioinformatics* **2013**, *29* (14), 1830−1831.
(21) Kyte, J.; Doolittle, R. F. A simple method for displaying the hydropathic character of a protein. *J. Mol. Biol.* **1982**, *157* (1), 105−32.
(22) Carvalho, L. B.; Capelo-Martínez, J. L.; Lodeiro, C.; Wiśniewski, J. R.; Santos, H. M. Ultrasonic-Based Filter Aided Sample Preparation as the General Method to Sample Preparation in Proteomics. *Analytical chemistry* **2020**, *92* (13), 9164−9171.
(23) Murillo, J. R.; Kuras, M.; Rezeli, M.; Milliotis, T.; Betancourt, L.; Marko-Varga, G. Automated phosphopeptide enrichment from minute quantities of frozen malignant melanoma tissue. *PloS one* **2018**, *13* (12), e0208562.
(24) Post, H.; Penning, R.; Fitzpatrick, M. A.; Garrigues, L. B.; Wu, W.; MacGillavry, H. D.; Hoogenraad, C. C.; Heck, A. J.; Altelaar, A. F. Robust, Sensitive, and Automated Phosphopeptide Enrichment Optimized for Low Sample Amounts Applied to Primary Hippocampal Neurons. *J. Proteome Res.* **2017**, *16* (2), 728−737.
(25) Pagel, O.; Loroch, S.; Sickmann, A.; Zahedi, R. P. Current strategies and findings in clinically relevant post-translational modification-specific proteomics. *Expert review of proteomics* **2015**, *12* (3), 235−53.
(26) Tremblay, T. L.; Hill, J. J. Adding polyvinylpyrrolidone to low level protein samples significantly improves peptide recovery in FASP digests: An inexpensive and simple modification to the FASP protocol. *Journal of proteomics* **2021**, *230*, 104000.
(27) Erde, J.; Loo, R. R.; Loo, J. A. Enhanced FASP (eFASP) to increase proteome coverage and sample recovery for quantitative proteomic experiments. *J. Proteome Res.* **2014**, *13* (4), 1885−95.
(28) Stadlmann, J.; Hudecz, O.; Krššáková, G.; Ctortecka, C.; Van Raemdonck, G.; Op De Beeck, J.; Desmet, G.; Penninger, J. M.; Jacobs, P.; Mechtler, K. Improved Sensitivity in Low-Input Proteomics Using Micropillar Array-Based Chromatography. *Analytical chemistry* **2019**, *91* (22), 14203−14207.
(29) Vistain, L. F.; Tay, S. Single-Cell Proteomics. *Trends in biochemical sciences* **2021**, *46*, 661.
(30) Martens, L.; Hermjakob, H.; Jones, P.; Adamski, M.; Taylor, C.; States, D.; Gevaert, K.; Vandekerckhove, J.; Apweiler, R. PRIDE: the proteomics identifications database. *Proteomics* **2005**, *5* (13), 3537−45.
(31) Sharma, V.; Eckels, J.; Schilling, B.; Ludwig, C.; Jaffe, J. D.; MacCoss, M. J.; MacLean, B. Panorama Public: A Public Repository for Quantitative Data Sets Processed in Skyline. *Molecular & cellular proteomics: MCP* **2018**, *17* (6), 1239−1244.

https://doi.org/10.1021/acs.jproteome.1c00706
J. Proteome Res. 2022, 21, 1181−1188